Hyperfine structure and Zeeman tuning of the $A\ ^2\Pi$–$X\ ^2\Sigma^+(0,0)$ band system of the odd isotopologue of strontium monofluoride ^{87}SrF

Anh T. Le, Hailing Wang, and Timothy C. Steimle
Department of Chemistry and Biochemistry, Arizona State University, Tempe, Arizona 85287-1604, USA
(Received 24 September 2009; published 15 December 2009)

The low-rotational lines of the $A\ ^2\Pi$-$X\ ^2\Sigma^+(0,0)$ band system of the odd isotopologue of strontium monofluoride, ^{87}SrF, were recorded and analyzed. The ^{87}Sr($I=9/2$) magnetic hyperfine interaction is significant only in the $|\Omega|=1/2$ spin-orbit component of the $A\ ^2\Pi$ state. Optical transitions appropriate for monitoring ultracold samples of ^{87}SrF are identified. The determined fine-structure parameters were used to predict the anisotropic magnetic g factor, g_l, for the $X\ ^2\Sigma^+(v=0)$ state. The g factors were used to predict the magnetic tuning of the $N=0$ (+parity) and $N=1$ (−parity) levels of the $X\ ^2\Sigma^+(v=0)$ state. A comparison to spectroscopic parameters for the ^{88}SrF isotopologue is given.

DOI: 10.1103/PhysRevA.80.062513 PACS number(s): 33.20.Kf

I. INTRODUCTION

There is renewed interest in the spectroscopy of heavy metal containing polar radical diatomic molecules because they provide a sensitive venue for detection of parity nonconservation (PNC) either from the determination of the electric-dipole moment (EDM) of the electron, d_e, or detection of the interaction of the anapole moment of the nuclei with the unpaired electron [1,2]. The effective Hamiltonian operator for a $X\ ^2\Sigma^+$ electronic state, including the PNC relevant terms, is [2,3]

$$\mathbf{H}^{eff}(^2\Sigma) = B\mathbf{N}^2 + \gamma\mathbf{N}\cdot\mathbf{S} + b_F(^{87}\mathrm{Sr},^{19}\mathrm{F})\mathbf{I}\cdot\mathbf{S} + c(^{87}\mathrm{Sr},^{19}\mathrm{F}) \times\left(I_zS_z - \frac{1}{3}\mathbf{I}\cdot\mathbf{S}\right) + eq_0Q(^{87}\mathrm{Sr})\frac{3I_z-\mathbf{I}^2}{4I(2I-1)} + W_Ak_A\mathbf{n}\times\mathbf{I}\cdot\mathbf{S} + (W_Sk_S + W_dd_e)\mathbf{S}\cdot\mathbf{n}, \quad (1)$$

where $\mathbf{N}$ is the angular-momentum operator excluding electronic spin, $\mathbf{S}$, and nuclear spin, $\mathbf{I}$, and $\mathbf{n}$ is a unit vector along the bond. The first five terms in Eq. (1) are commonly used to model the fine (via the B and γ terms), Fermi contact and dipolar magnetic hyperfine (via the b_F and c terms), and the electric-quadrupole hyperfine (via the eq_0Q term) interactions. The last three terms account for the very small energy contributions due to the P- and P,T-odd PNC effects. The first term describes the interaction of the anapole moment of the nucleus, k_A, with the electron spin, the second a scalar electron-nucleus interaction, and the third the interaction of d_e with the effective electric field, W_d.

Most of the previous theoretical [3–6] and experimental [7–9] efforts related to PNC have focused on the determination of d_e. The effects due to d_e are nuclear spin independent and studies of both even and odd nuclear spin isotopologues are relevant. Recently, DeMille *et al.* [10] proposed using the odd isotopologues of strontium monofluoride, ^{87}SrF, and other heavy transition metal diatomic molecules to measure the nuclear spin-dependent parity nonconservation (NSD-PNC) effect resulting from the interaction of the anapole moment of ^{87}Sr with the unpaired electron of the $X\ ^2\Sigma^+$ electronic state. In the proposed experimental scheme, the $N=0$ (+parity) levels of the ground vibronic $X\ ^2\Sigma^+(v=0)$ state would be magnetically tuned into near degeneracy with the $N=1$ (−parity) levels. The nearly degenerate levels are mixed by NSD-PNC interactions. A laser-induced fluorescence detection scheme using the $A\ ^2\Pi - X\ ^2\Sigma^+(0,0)$ band system is proposed; consequently, a spectroscopic understanding of the energy levels of both the $A\ ^2\Pi(v=0)$ and $X\ ^2\Sigma^+(v=0)$ states for the ^{87}SrF isotopologue is required in support of proposed NSD-PNC experiments.

The magnetic hyperfine interaction in the $X\ ^2\Sigma^+(v=0)$ vibronic state of ^{87}SrF derived from spectroscopic investigations is also relevant to the interpretation of the PNC measurements. Specifically, the W_i constants of the PNC terms in Eq. (1) mostly depend upon a knowledge of electron spin density in the vicinity of the heavy nucleus; $\langle\Psi^{el}|\Sigma_i\delta(r_i)|\Psi^{el}\rangle$. Similarly, the Fermi contact magnetic hyperfine interaction is also dependent on $\langle\Psi^{el}|\Sigma_i\delta(r_i)|\Psi^{el}\rangle$. Thus, experimentally derived values for the magnetic hyperfine parameters are used either as a test of *ab initio* electronic calculations of W_i constants [2,11–13] or as input into semiempirical predictions of the W_i constants [14]. Here we report on the analysis of the hyperfine structure of the $A\ ^2\Pi - X\ ^2\Sigma^+(0,0)$ band of ^{87}SrF. The magnetic tuning of the $N=0$ (+parity) and $N=1$ (−parity) levels of the $X\ ^2\Sigma^+(v=0)$ state is also predicted.

The main isotopologue of strontium monofluoride, ^{88}SrF, has been extensively studied by visible [15–21], infrared [22], microwave [23,24], and rf [25] spectroscopies. The only reported spectroscopic investigation of ^{87}SrF is the rf-double resonance study by Azuma *et al.* [26]. In that study, magnetic dipole-allowed transitions between the spin-rotation components of high-rotational levels ($N>39$) were precisely measured and analyzed to produce hyperfine and spin-rotation parameters for the $X\ ^2\Sigma^+(v=0)$ state. The ^{87}Sr magnetic hyperfine parameters were within a few percent of those determined from the analysis of the matrix-isolated electron-spin resonance (ESR) spectrum [27]. There has been no previous characterization of the low rotational levels of the $X\ ^2\Sigma^+(v=0)$ state or any levels of the $A\ ^2\Pi(v=0)$ state.

II. EXPERIMENTAL

The supersonic molecular beam production and laser-induced fluorescent detection schemes are identical to those

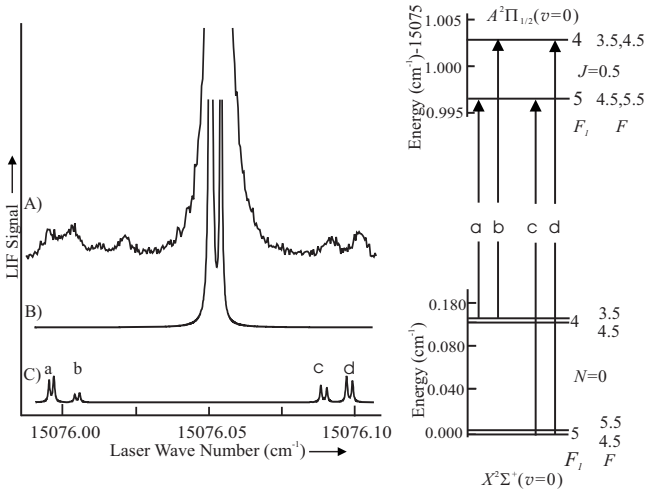

FIG. 1. The (A) observed and [(B) and (C)] calculated spectra in the region of the ${}^{Q}Q_{14}(0)$ (ν=15 076.00 cm^{-1}) and the ${}^{Q}Q_{15}(0)$ (ν=15 076.99 cm^{-1}) branch features of the ^{87}SrF and associated energy level pattern. The intense spectral feature is an overlap of ${}^{Q}Q_{11}(0)$ lines of ^{88}SrF and ^{86}SrF. The predicted spectrum for the ^{87}SrF isotopologue (C) was obtained using the optimized set of parameters given in Table II and that of ^{88}SrF (B) using the parameters of Ref. [20]. A line width of 10 MHz was used in the predicted spectra. Splitting due to the magnetic hyperfine interaction in the $A\ {}^2\Pi_{1/2}(v=0)$ state is evident.

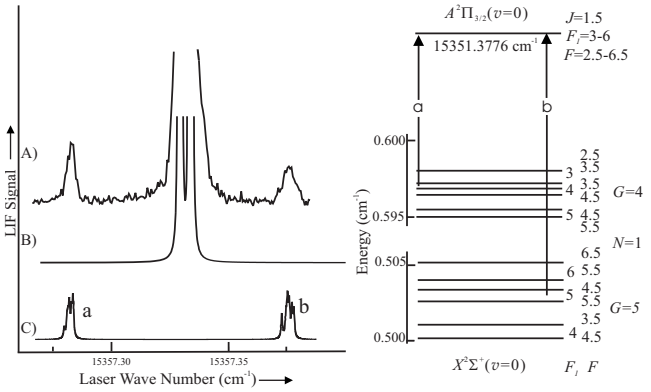

FIG. 2. The (A) observed and [(B) and (C)] calculated spectra in the region of the ${}^{R}Q_{24}(1)$ (ν=15 357.28 cm^{-1}) and the ${}^{R}Q_{24}(1)$ (ν=15 357.38 cm^{-1}) branch features of the ^{87}SrF and associated energy level pattern. The intense spectral feature is an overlap of ${}^{R}R_{22}(1)$ and ${}^{R}Q_{21}(1)$ lines of ^{88}SrF and ^{86}SrF. The predicted spectrum for the ^{87}SrF isotopologue (C) was obtained using the optimized set of parameters given in Table II and that of ^{88}SrF (B) using the parameters of Ref. [20]. A line width of 10 MHz was used in the predicted spectra. There is no evidence of $A\ {}^2\Pi_{3/2}(v=0)$ magnetic hyperfine splitting.

used in the previous field-free measurements of ^{88}SrF [20]. A continuously rotating strontium metal rod was ablated in a supersonic expansion of approximately 5% sulfur hexafluoride (SF_6) seeded in argon carrier gas with a backing pressure of approximately 3 MPa. The pulsed free jet expansion was skimmed to form a well-collimated molecular beam which was crossed with a single longitudinal mode, continuous wave dye laser approximately 50 cm downstream from the source. The laser power was attenuated to approximately 10 mW and lightly focused to avoid power broadening. Spectral line widths of less than 40 MHz full width at half maximum were observed.

The absolute wave numbers were determined to an accuracy ± 0.001 cm^{-1} by simultaneously recording the sub-Doppler I_2 absorption spectrum [28,29]. Extrapolation between I_2 absorption features was achieved by simultaneously recording the transmission of two confocal étalons. One étalon was actively stabilized and calibrated to have a free spectral range of 749.14 MHz. A second, unstabilized étalon with a free spectral range of 75.7 MHz was used to interpolate between transmission peaks of the stabilized étalon.

III. OBSERVATIONS

There are four naturally occurring isotopes of Sr: ^{84}Sr(0.6%), ^{86}Sr(9.9%), ^{87}Sr(7.0%), and ^{88}Sr(82.5%). The observed and calculated laser-induced fluorescence (LIF) spectrum in the region of the ${}^{Q}Q_{11}(0)$ branch feature (ν =15 076.05 cm^{-1}) of the $A\ {}^2\Pi_{1/2}-X\ {}^2\Sigma^+(0,0)$ subband system of ^{88}SrF is given in Fig. 1. The associated energy levels and assigned transitions for ^{87}SrF, as predicted from the final analysis (*vide infra*), are also given in Fig. 1. The intense spectral feature is a blend of the ^{86}SrF and ^{88}SrF isotopologues which is readily identified from the previous analysis [20]. The weaker pair of doublets that straddle the main feature is due to the ^{87}SrF isotopologue. The observed and calculated spectra in the region of the ${}^{R}R_{22}(1)$ branch feature (ν=15 357.34 cm^{-1}) of the $A\ {}^2\Pi_{3/2}-X\ {}^2\Sigma^+(0,0)$ subband system of ^{88}SrF are given in Fig. 2. The associated energy levels and assigned transitions for ^{87}SrF, as predicted from the final analysis (*vide infra*), are also given in Fig. 2. Again, the intense feature is a blend of the ^{86}SrF and ^{88}SrF isotopologues, with the ^{86}SrF feature being partially resolved. The weaker two features that startle the main feature are due to the ^{87}SrF isotopologue. The spectral features due to the ^{87}SrF isotopologue are markedly different from those due to the ^{86}SrF and ^{88}SrF isotopologues because the nonzero nuclear magnetic moment of ^{87}Sr(I=9/2)(μ=−1.092 83μ_N) results in a large magnetic hyperfine splitting in the $X\ {}^2\Sigma^+$ state [26]. The ^{87}Sr (and ^{19}F) magnetic hyperfine interaction is relatively small in the $A\ {}^2\Pi$ state (*vide infra*). As indicated in the energy level diagram of Fig. 2, there are numerous unresolved transitions associated with each of the doublets. The observed and calculated transition wave number and associated quantum number assignment for the ^{87}SrF isotopologue are listed in Table I. The difference between the measured and predicted transition wave number based on the final optimized parameters is also given in Table I. A total of 75 optical transitions was precisely measured: 40 in the $A\ {}^2\Pi_{3/2}-X\ {}^2\Sigma^+(0,0)$ subband and 35 in the $A\ {}^2\Pi_{1/2}-X\ {}^2\Sigma^+(0,0)$ subband.

IV. APPEARANCE OF THE SPECTRUM

The energy level patterns for the low rotational levels of the $X\ {}^2\Sigma^+$ state of the even Sr isotopologues are those of a molecule near the Hund's case ($b_{\beta J}$) limit with the approxi-

TABLE I. Observed and calculated line positions of the $A\ ^2\Pi - X\ ^2\Sigma^+(0,0)$ band system of ^{87}SrF.[a]

Branch	$F_1'', F''-F_1', F'$	Observed −15 000	Obs-calc	Branch	$F_1'', F''-F_1', F'$	Observed −15 000	Obs-calc
$^SR_{24}(0)$	4.0, 3.5–5.0, 4.5	357.7836	0.0002	$^PP_{14}(1)$	3.0,2.5–4.0, 4.5	75.6260	0.0003
$^SR_{25}(0)$	5.0, 4.5–6.0, 5.5	357.8787	0.0010		4.0,4.5–5.0,5.5	75.6340	−0.0005
$^QP_{24}(2)$	6.0, 6.5–5.0, 5.5	356.2794	−0.0008	$^PP_{15}(1)$	5.0,5.5–4.0, 4.5	75.7261	0.0026
$^QP_{25}(2)$	6.0, 6.5–6.0, 6.5	356.3744	0.0028	$^QQ_{14}(0)$	4.0,4.5–5.0,5.5	75.9997	0.0017
$^RQ_{24}(1)$	5.0, 5.5–6.0, 6.5	357.2824	−0.0001		4.0,4.5–4.0, 4.5	76.0072	0.0029
$^RQ_{25}(1)$	5.0, 5.5–6.0, 6.5	357.3737	−0.0025	$^QQ_{15}(0)$	5.0,5.5–5.0,5.5	76.0890	−0.0013
$^RQ_{24}(10)$	9.0, 9.5–9.0, 9.5	359.9101	−0.0016		5.0,5.5–4.0, 4.5	76.0980	−0.0005
	12.0, 12.5–12.0, 12.5	359.9201	0.0001	$^RR_{14}(0)$	4.0,4.5–5.0,5.5	76.9584	−0.0009
	13.0, 13.5–13.0, 13.5	359.9232	0.0000	$^RR_{15}(1)$	6.0, 6.5–7.0, 7.5	77.8853	−0.0029
	14.0, 14.5–14.0, 14.5	359.9269	0.0002	$^RR_{14}(2)$	5.0, 4.5–5.0, 4.5	78.6294	−0.0008
$^RQ_{25}(10)$	15.0, 15.5–15.0, 15.5	359.9964	−0.0007	$^RR_{15}(2)$	7.0, 7.5–8.0, 8.5	78.7257	0.0006
	14.0, 14.5–14.0, 14.5	360.0022	−0.0014	$^QQ_{14}(4)$	8.0, 8.5–9.0, 9.5	76.8021	−0.0008
	13.0, 12.5–13.0, 12.5	360.0072	−0.0021	$^QQ_{15}(4)$	9.0, 9.5–9.0, 9.5	76.8862	0.0003
	9.0, 8.5–9.0, 8.5	360.0174	−0.0021		7.0, 7.5–7.0, 7.5	76.8964	−0.0002
	14.0, 14.5–14.0, 14.5	360.0243	0.0012		5.0, 4.5–5.0, 4.5	76.9039	0.0006
$^RQ_{24}(11)$	9.0, 8.5–9.0, 8.5	360.2363	0.0005	$^QQ_{14}(10)$	6.0, 5.5–6.0, 5.5	78.1697	0.0008
	12.0, 12.5–12.0, 12.5	360.2433	0.0002		13.0,12.5–14.0,13.5	78.1784	0.0005
	13.0, 13.5–13.0,13.5	360.2463	0.0000	$^QQ_{15}(10)$	15.0,15.5–15.0,15.5	78.2523	0.0014
	14.0, 14.5–14.0,14.5	360.2503	0.0006		14.0,14.5–14.0,14.5	78.2585	−0.0003
	15.0, 15.5–15.0,15.5	360.2534	−0.0003		13.0,13.5–13.0,13.5	78.2649	−0.0002
$^RQ_{25}(11)$	15.0, 15.5–15.0, 15.5	360.3295	0.0005		12.0,12.5–12.0,12.5	78.2696	−0.0007
	14.0, 14.5–14.0, 14.5	360.3341	−0.0004	$^QQ_{14}(11)$	7.0, 7.5–7.0, 7.5	78.4172	0.0017
	8.0, 8.5–8.0, 8.5	360.3504	0.0001		15.0,15.5–16.0,16.5	78.4302	−0.0001
$^RQ_{24}(12)$	9.0, 9.5–9.0, 9.5	360.5663	0.0017	$^QQ_{15}(11)$	16.0,16.5–16.0,16.5	78.5006	0.0019
	12.0, 12.5–12.0, 12.5	360.5710	−0.0018		15.0,15.5–15.0,15.5	78.5069	−0.0001
	14.0, 14.5–14.0, 14.5	360.5797	0.0003		14.0,14.5–14.0,14.5	78.5126	−0.0010
	15.0, 15.5–15.0, 15.5	360.5838	0.0010		13.0,13.5–13.0,13.5	78.5169	−0.0022
	16.0, 16.5–16.0, 16.5	360.5880	−0.0003	$^QQ_{15}(12)$	16.0,16.5–16.0,16.5	78.7602	−0.0009
$^RQ_{25}(12)$	15.0, 15.5–15.0, 15.5	360.6676	0.0005		15.0,15.5–15.0,15.5	78.7679	−0.0002
	14.0, 14.5–14.0, 14.5	360.6718	0.0000		14.0,14.5–14.0,14.5	78.7730	−0.0009
	13.0, 13.5–13.0, 13.5	360.6752	−0.0003		13.0,13.5–13.0,13.5	78.7914	−0.0004
	12.0, 12.5–12.0, 12.5	360.6781	−0.0004	$^QQ_{15}(13)$	16.0,16.5–16.0,16.5	79.0289	0.0002
	8.0, 8.5–8.0, 8.5	360.6846	0.0007		15.0,15.5–15.0,15.5	79.0344	−0.0003
$^RQ_{24}(13)$	18.0, 18.5–18.0, 18.5	360.9932	0.0007		13.0,13.5–13.0,13.5	79.0384	−0.0009
	17.0, 17.5–17.0, 17.5	361.0016	0.0011		9.0,9.5–9.0,9.5	79.0549	0.0009
	16.0, 16.5–16.0, 16.5	361.0072	0.0005				
	15.0, 15.5–15.0, 15.5	361.0115	−0.0002		Std. Dev.=0.0012 cm^{-1}		
	14.0, 14.5–14.0, 14.5	361.0149	−0.0007				
	13.0, 13.5–13.0, 13.5	361.0177	−0.0011				
$^RQ_{25}(13)$	9.0, 9.5–9.0, 9.5	361.0257	0.0019				

[a]The differences between the observed and calculated values were obtained using the spectroscopic parameters of Table II for the excited state. The parameters for the $X\ ^2\Sigma^+$ were held fixed to those of Ref. [26]. All units are in wave numbers, cm^{-1}.

mately good intermediate quantum number being J resulting from coupling the rotational angular momentum, **N**, with the electron spin angular momentum, **S**. The ^{19}F ($I=1/2$) hyperfine interaction is small and each rotational level of a given J of the even isotopologues splits into two levels designated by the total angular momentum F. The resulting Hund's case ($b_{\beta J}$) vector coupling appropriate for the even isotopologues can be written as

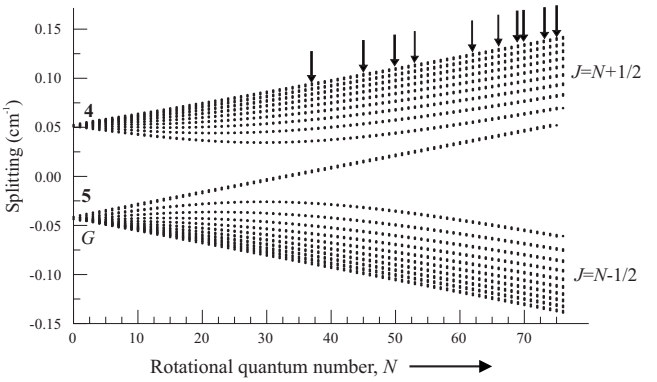

FIG. 3. The ^{87}SrF isotopologue spin-rotation and hyperfine energy levels pattern for the $X\ ^2\Sigma^+(v=0)$ state as a function of rotational quantum number, N. The previously measured rf transitions (Ref. [26]) are indicated by arrows. The low-rotational levels are those of a Hund's case ($b_{\beta S}$) and those of the high rotational levels a Hund's case ($b_{\beta J}$).

$$\mathbf{S}+\mathbf{N}=\mathbf{J};\quad \mathbf{I_1}(^{19}\mathrm{F})+\mathbf{J}=\mathbf{F}, \tag{2}$$

which corresponds to the basis set $|\eta\Lambda\rangle|(SN)J(JI_1)F\rangle$.

The large ^{87}Sr magnetic hyperfine interaction in the $X\ ^2\Sigma^+$ state causes the energy level pattern for the low rotational levels of the ^{87}SrF isotopologue to be that of a molecule near the Hund's case ($b_{\beta S}$) limit with the approximately good intermediate quantum number being G (=4 and 5) resulting from coupling the ^{87}Sr nuclear spin angular momentum, $\mathbf{I_1}$, with the total electron spin angular momentum, $\mathbf{S}$. The ^{19}F nuclear spin is weakly coupled to $\mathbf{G}$ to produce the total angular momentum, $\mathbf{F}$. The Hund's case ($b_{\beta S}$) vector coupling for low rotational levels can be written as

$$\mathbf{S}+\mathbf{I_1}(^{87}\mathrm{Sr})=\mathbf{G}(^{87}\mathrm{Sr});\quad \mathbf{N}+\mathbf{G}(^{87}\mathrm{Sr})=\mathbf{F}_1;$$
$$\mathbf{F}_1+\mathbf{I_2}(^{19}\mathrm{F})=\mathbf{F}, \tag{3}$$

which corresponds to the basis function $|\eta\Lambda\rangle|(SI_1)G(GN)F_1(F_1I_2)F\rangle$. The energy level pattern of the $X\ ^2\Sigma^+(v=0)$ state of ^{87}Sr($I=9/2$) as a function of rotation, predicted using the previously determined fine and hyperfine parameters [26], is illustrated in Fig. 3. The contribution due to rotation [$\approx BN(N+1)$] has been subtracted to emphasize the spin-rotation and hyperfine contributions. As illustrated in Fig. 3, the electron spin $\mathbf{S}$ uncouples from $\mathbf{I_1}$ (^{87}Sr) with increasing rotation and recouples to $\mathbf{N}$. The energy level patterns of the high rotational levels of the $X\ ^2\Sigma^+$ state of ^{87}SrF, which were previously studied [26], are those of a molecule near the sequentially coupled Hund's case ($b_{\beta J}$) limit. The vector coupling can be written as

$$\mathbf{S}+\mathbf{N}=\mathbf{J};\quad \mathbf{I_1}(^{87}\mathrm{Sr})+\mathbf{J}=\mathbf{F}_1;\quad \mathbf{F}_1+\mathbf{I_2}(^{19}\mathrm{F})=\mathbf{F}, \tag{4}$$

which corresponds to the basis function $|\eta\Lambda\rangle|(SN)J(JI_1)F_1(F_1I_2)F\rangle$.

A conventional $^2\Pi$(case $a_{\beta J}$)-$^2\Sigma^+$(case $b_{\beta J}$) labeling scheme of $^{\Delta N}\Delta J_{F_i'F_i''}(N'')$ [30], where F_i'' and F_i' subscripts designate the spin component of the $X\ ^2\Sigma^+$ and $A\ ^2\Pi$ states, respectively, is appropriated for the even isotopologues and transitions involving high-rotational levels of ^{87}SrF. In this case, the first subscript, F_i', $i=1$, for the $A\ ^2\Pi_{1/2}$ component and $i=2$ for $A\ ^2\Pi_{3/2}$ component and the second subscript, F_i'', $i=1$ or 2, for $J=N+1/2$ or $N-1/2$, respectively. The intermediate quantum number J is not appropriate for the low rotational levels for the $X\ ^2\Sigma^+$ state of ^{87}SrF and hence neither is the "F_i''" subscript in the conventional $^2\Pi$(case $a_{\beta J}$)-$^2\Sigma^+$(case $b_{\beta J}$) branch designation. It is customary to replace F_i'' with the intermediate approximately good quantum number G'' of the Hund's case ($b_{\beta S}$) coupling scheme. The 12 branches of the $^2\Pi$(case $a_{\beta J}$)-$^2\Sigma^+$(case $b_{\beta J}$) labeling scheme ($^PP_{11}$, $^QQ_{11}$, $^RR_{11}$, $^PQ_{12}$, $^OP_{12}$, $^QR_{12}$, $^PP_{22}$, $^QQ_{22}$, $^RR_{22}$, $^RQ_{21}$, $^QP_{21}$, and $^SR_{21}$) [30] regroup into 16 branch features of the $^2\Pi$(case $a_{\beta J}$)-$^2\Sigma^+$(case $b_{\beta S}$) scheme. The branches are designated as $^OP_{1G}$, $^PP_{1G}+^PQ_{1G}$, $^QQ_{1G}+^QR_{1G}$, and $^RR_{1G}$ for the $^2\Pi_{1/2}$(case $a_{\beta J}$)-$^2\Sigma^+$(case $b_{\beta S}$) subband and $^PP_{2G}$, $^QP_{2G}+^QQ_{2G}$, $^RQ_{2G}+^RR_{2G}$, and $^SR_{2G}$ for the $^2\Pi_{3/2}$(case $a_{\beta J}$)-$^2\Sigma^+$(case $b_{\beta S}$) subband with $G=4$ and 5. The abbreviations $^PP_{1G}$, $^QQ_{1G}$, $^QP_{2G}$, and $^RQ_{2G}$ will be used for the $^PP_{1G}+^PQ_{1G}$, $^QQ_{1G}+^QR_{1G}$, $^QP_{2G}+^QQ_{2G}$, and $^RQ_{2G}+^RR_{2G}$ branches, respectively.

V. ANALYSIS

A direct fit to the measured transition wave numbers given in Table I was performed. The effective Hamiltonian for the $X\ ^2\Sigma^+(v=0)$ state was taken as the first five terms in Eq. (1) augmented by the centrifugal distortion correction to the rotation, D. The centrifugal distortion corrections to the magnetic hyperfine parameters for the $X\ ^2\Sigma^+(v=0)$ state, derived from the analysis of the rf spectrum of the high rotational levels [26], were not required because only optical transitions involving low rotational levels were measured. The energies of the $X\ ^2\Sigma^+(v=0)$ state were determined by numerical diagonalization of a Hamiltonian matrix representation of dimension $40[=(2S+1)(2I_1+1)(2I_2+1)]$ constructed in a sequentially coupled, nonparity, Hund's case ($a_{\beta J}$) basis set. Expressions for the matrix elements were taken from Ref. [31]. Combination and difference revealed that only the e-parity components in the $A\ ^2\Pi_{1/2}(v=0)$ subband exhibited magnetic hyperfine splitting. Therefore, the energies for the $A\ ^2\Pi(v=0)$ state were modeled by including the origin ($T_{0,0}$), spin-orbit interaction (A), rotation (B), and associated centrifugal distortion correction (D), the Λ-doubling ($p+2q$), and magnetic hyperfine the Λ-type magnetic hyperfine $d(^{87}\mathrm{Sr})$ interaction terms [31]

$$\mathbf{H}^{\mathrm{eff}}(^2\Pi)=T_{0,0}+AL_zS_z+B\mathbf{R}^2-D(\mathbf{R}^2)^2$$
$$+\frac{1}{2}(p+2q)(e^{-2i\phi}J_+S_++e^{+2i\phi}J_-S_-)$$
$$+\frac{1}{2}d(e^{-2i\phi}I_+S_++e^{+2i\phi}I_-S_-). \tag{5}$$

In Eq. (5), $J_\pm$, $S_\pm$, and $I_\pm$ are the shift operators of the total angular momentum in the absence of nuclear spin, $\mathbf{J}$, the total electron spin, $\mathbf{S}$, and the ^{87}Sr nuclear spin angular momentum, $\mathbf{I_1}$, and ϕ is the azimuthal coordinate of the electrons. The energies of the $A\ ^2\Pi(v=0)$ state were determined by numerical diagonalization of a Hamiltonian matrix repre-

TABLE II. The determined spectroscopic parameters for the $A\ ^2\Pi(v=0)$ state of ^{87}SrF.[a]

Parameter[a]	Fitted values[b]	Scaled values[c]	Correlation matrix[d]				
A	281.4615(8)	281.459(2)	1.00				
B	0.253762(5)	0.25387(3)	−0.702	1.00			
$p+2q$	−0.13333(16)	−0.130(1)	0.821	−0.716	1.00		
d	−0.00187(20)		−0.028	0.085	−0.128	1.00	
T_{00}	15216.5954(5)	15216.6016(20)	0.318	−0.757	0.251	−0.094	1.00

[a]The γ, eq_0Q, $b_F(^{87}\mathrm{Sr})$, $c(^{87}\mathrm{Sr})$, $b_F(^{19}\mathrm{F})$, and $c(\mathrm{F})$ parameters of the $X\ ^2\Sigma^+(v=0)$ state were constrained values in Ref. [26] and B of the $X\ ^2\Sigma^+(v=0)$ state to 0.250 268 0 cm^{-1}.
[b]All units in wave numbers (cm^{-1}). Numbers in parentheses represent a 2σ error estimate in the last quoted decimal point.
[c]The values obtained by scaling the values for ^{88}SrF given in Ref. [20] by the isotopic dependence.
[d]Elements of correlation matrix given in the order in which the parameters are presented.

sentation of dimension $80[=2(2S+1)(2I_1+1)(2I_2+1)]$ constructed in sequentially coupled, nonparity, Hund's case ($a_{\beta J}$) basis set. Expressions for the matrix elements were taken from Ref. [31]. The basis set for the $A\ ^2\Pi(v=0)$ state spanned the space of the ^{19}F nuclear spin, $\mathbf{I}_2$, even though the effect was not resolved in the spectra in order to facilitate intensity predictions.

Predicted transition wave numbers were obtained from the appropriate combinations of the calculated ground and excited state energies and used, along with the measured transition wave numbers of Table I, as input into a nonlinear least-squares fitting program. Fits using various combinations of ground and excited state parameters were performed. In the end, satisfactory modeling of the spectrum could be achieved by optimizing only the $T_{0,0}$, A, B, $p+2q$, and $d(^{87}\mathrm{Sr})$ parameters of the $A\ ^2\Pi(v=0)$ state. In this final fit, the γ, eq_0Q, $b_F(^{87}\mathrm{Sr})$, $c(^{87}\mathrm{Sr})$, $b_F(^{19}\mathrm{F})$, and $c(^{19}\mathrm{F})$ parameters of the $X\ ^2\Sigma^+(v=0)$ state were constrained to the values determined from the analysis of the spin-rotation transitions of the high rotational levels [26]. The rotational parameter, B, of the $X\ ^2\Sigma^+(v=0)$ state was constrained to 0.250 268 0 cm^{-1}, which is predicted by isotopic scaling: $B(^{87}\mathrm{SrF})=B(^{88}\mathrm{SrF})[\mu(^{88}\mathrm{SrF})/\mu(^{87}\mathrm{SrF})]$. The centrifugal distortion correction to the rotation parameters, D, for the $X\ ^2\Sigma^+(v=0)$ and $A\ ^2\Pi(v=0)$ states were constrained to the values determined for ^{88}SrF [20]. The optimized parameters, associated errors, and correlation matrix are given in Table II. The standard deviation of the fit is 0.0012 cm^{-1}, which is commensurate with the measurement uncertainty.

VI. DISCUSSION

The transition wave numbers of the low-rotational lines of the $A\ ^2\Pi-X\ ^2\Sigma^+(0,0)$ band system of the odd isotopologue of strontium monofluoride, ^{87}SrF, have been accurately determined and analyzed to produce the first set of molecular parameters for the $A\ ^2\Pi(v=0)$ state. The fine-structure parameters determined from the analysis of the magnetic dipole-allowed rf transition within high rotational levels [26] of the $X\ ^2\Sigma^+(v=0)$ state have been shown to accurately predict the energy levels of the low rotational levels proposed to be used in a NSD-PNC experiment [10]. The newly determined parameters can accurately model the $A\ ^2\Pi-X\ ^2\Sigma^+(0,0)$ spectrum as illustrated in Figs. 1 and 2 where the predicted spectra are presented. The small splitting of the $^QQ_{14}(0)$ ($\nu=15\ 076.00\ \mathrm{cm}^{-1}$) and the $^QQ_{15}(0)$ ($\nu=15\ 076.99\ \mathrm{cm}^{-1}$) branch features of Fig. 1 are due to the magnetic hyperfine interaction in the $A\ ^2\Pi_{1/2}(v=0)$ state. The $^QQ_{15}(0)$ ($\nu=15\ 076.99\ \mathrm{cm}^{-1}$) branch feature is optimum for monitoring an ultracold sample ^{87}SrF because this transition has as the lowest terminus the ground quantum state, the hyperfine structure is resolved, and the spectrum is not overlapped.

The T_{00}, A, B, and $p+2q$ parameters for the ^{88}SrF isotopologue are (in cm^{-1}) [20] 15 216.596(2), 281.459(2), 0.252 84(3), and −0.130(1), respectively. Listed in Table II are the values of T_{00}, A, B, and $p+2q$ obtained by scaling the ^{88}SrF parameters by the known isotopic relationships [31]. The vibrational parameters of Ref. [32] were used to obtain

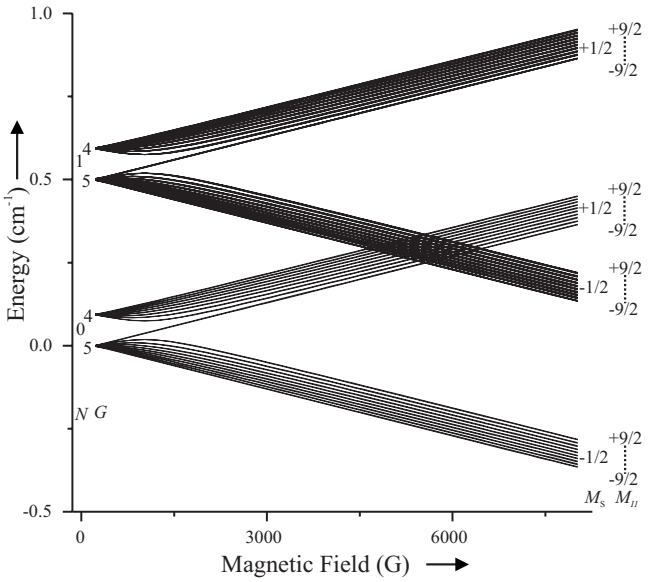

FIG. 4. The magnetic tuning of the $N=0$ (+parity) and $N=1$ (−parity) levels of the $X\ ^2\Sigma^+(v=0)$ state of ^{87}SrF. The pattern was obtained using the field-free hyperfine and spin-rotation parameters of Ref. [26], a rotational constant, B, of 0.250 268 0 cm^{-1} (see text), $g_S=2.002$, and $g_l=-0.005$.

the predicted T_{00} value. The predicted T_{00} and B values differ slightly from the fitted values because of nonadiabatic contributions. An *a priori* prediction of the magnetic hyperfine parameters for the $A\ ^2\Pi(v=0)$ state is not possible. The relatively large d magnetic hyperfine parameter is consistent with the large Λ-doubling parameter $(p+2q)$, which is due to the interaction with the nearby $B\ ^2\Sigma^+$ state.

In the proposed NSD-PNC experiment [10], the $N=0$ (+parity) levels of the ground vibronic $X\ ^2\Sigma^+(v=0)$ state would be magnetically tuned into near degeneracy with the $N=1$ (−parity) levels. The predicted magnetic tuning of the low-N rotational lines for the $X\ ^2\Sigma^+$ states of the ^{87}SrF isotopologue is given in Fig. 4. The prediction was performed by ignoring the small contributions from rotation and nuclear spin, and taking the effective Zeeman Hamiltonian for the $X\ ^2\Sigma^+(v=0)$ state as [31,33]

$$\mathbf{H}^{Zee}(eff) = g_S\mu_B\hat{\mathbf{S}}\cdot\hat{\mathbf{B}} + g_l\mu_B(\hat{S}_x\hat{B}_x + \hat{S}_y\hat{B}_y). \quad (6)$$

The eigenvalues and eigenvectors were obtained by constructing and numerically diagonalizing a 200×200 matrix representation $\mathbf{H}^{Zee}(eff)+\mathbf{H}^{\text{field-free}}(eff)$ constructed in a sequentially coupled Hund's case $(a_{\beta J})$ basis set for $F=2.5-6.5$. The expressions for the $\mathbf{H}^{Zee}(eff)$ matrix elements in a single nuclear spin Hund's case $(a_{\beta J})$ basis function, $|\eta\Lambda\rangle|S\Sigma\rangle|J\Omega(JI)F\rangle$, can be found in Ref. [31]. The expressions for the $\hat{\mathbf{H}}^{Zee}(eff)$ matrix elements in a two nuclear spin sequentially coupled Hund's case $(a_{\beta J})$ basis function, $|\eta\Lambda\rangle|S\Sigma\rangle|J\Omega(JI_1)F_1(F_1I_2)F\rangle$, are readily obtained using standard angular-momentum theory for coupling of the second nuclear spin [34]. The pattern was obtained using the field-free hyperfine and spin-rotation parameters of Ref. [26], a rotational constant, B, of 0.250 268 0 cm^{-1}, $g_S=2.002$, and $g_l=-0.005$. The $g_l=-0.005$ value was obtained using the Curl relationship [31]. The Zeeman tuning pattern for the $X\ ^2\Sigma^+$ state reveals that the approximately good quantum numbers at high magnetic field are $M_S(=\pm\frac{1}{2})$, $M_{I1}(^{87}\text{Sr})$ $(=\pm1/2,\ 3/2,\ 5/2,\ 7/2,$ and $9/2)$ and $M_{I2}(^{19}\text{F})$ $(=\pm\frac{1}{2})$, whereas at low and moderate fields, the approximately good quantum number is M_G. The $N=0$ (+parity) and $N=1$ (−parity) levels are magnetically tuned into near degeneracy over a magnetic field ranging from 4300 to 6200 G.

ACKNOWLEDGMENT

This research has been supported by the National Science Foundation–Experimental Physical Chemistry Grant No. 0646473.

[1] V. V. Flambaum and I. B. Khriplovich, Phys. Lett. A **110**, 121 (1985).
[2] M. G. Kozlov and L. N. Labzowsky, J. Phys. B **28**, 1933 (1995).
[3] M. G. Kozlov, A. V. Titov, N. S. Mosyagin, and P. V. Souchko, Phys. Rev. A **56**, R3326 (1997).
[4] M. G. Kozlov, J. Phys. B **30**, L607 (1997).
[5] M. G. Kozlov and D. DeMille, Phys. Rev. Lett. **89**, 133001 (2002).
[6] N. E. Shafer-Ray, Phys. Rev. A **73**, 034102 (2006).
[7] J. J. Hudson, B. E. Sauer, M. R. Tarbutt, and E. A. Hinds, Phys. Rev. Lett. **89**, 023003 (2002).
[8] D. Kawall, F. Bay, S. Bickman, Y. Jiang, and D. DeMille, Phys. Rev. Lett. **92**, 133007 (2004).
[9] P. Sivakumar, C. P. McRaven, D. Combs, N. E. Shafer-Ray, and V. Ezhov, Phys. Rev. A **77**, 062508 (2008).
[10] D. DeMille, S. B. Cahn, D. Murphree, D. A. Rahmlow, and M. G. Kozlov, Phys. Rev. Lett. **100**, 023003 (2008).
[11] A. V. Titov, N. S. Mosyagin, and V. F. Ezhov, Phys. Rev. Lett. **77**, 5346 (1996).
[12] N. S. Mosyagin, M. G. Kozlov, and A. V. Titov, J. Phys. B **31**, L763 (1998).
[13] A. V. Titov, N. S. Mosyagin, A. N. Petrov, and T. A. Isaev, Int. J. Quantum Chem. **104**, 223 (2005).
[14] M. G. Kozlov and V. F. Ezhov, Phys. Rev. A **49**, 4502 (1994).
[15] T. C. Steimle, P. J. Domaille, and D. O. Harris, J. Mol. Spectrosc. **68**, 134 (1977).
[16] J. M. Brown, D. J. Milton, and T. C. Steimle, Faraday Discuss. **71**, 151 (1981).
[17] W. E. Ernst and J. O. Schröder, Chem. Phys. **78**, 363 (1983).
[18] C. Nitsch, J. O. Schröder, and W. E. Ernst, Chem. Phys. Lett. **148**, 130 (1988).
[19] J. Kändler, T. Martell, and W. E. Ernst, Chem. Phys. Lett. **155**, 470 (1989).
[20] T. C. Steimle, D. A. Fletcher, and C. T. Scurlock, J. Mol. Spectrosc. **158**, 487 (1993).
[21] P. M. Sheridan, J.-G. Wang, M. J. Dick, and P. F. Bernath, J. Chem. Phys. A **113**, 13383 (2009).
[22] P. Colarusso, B. Guo, K.-Q. Zhang, and P. F. Bernath, J. Mol. Spectrosc. **175**, 158 (1996).
[23] H.-U. Schütze-Pahlmann, Ch. Ryzlewicz, J. Hoeft, and T. Törring, Chem. Phys. Lett. **93**, 74 (1982).
[24] W. E. Ernst, Appl. Phys. B: Lasers Opt. **30**, 105 (1983).
[25] W. J. Childs, L. S. Goodman, and I. Renhorn, J. Mol. Spectrosc. **87**, 522 (1981).
[26] Y. Azuma, W. J. Childs, G. L. Goodman, and T. C. Steimle, J. Chem. Phys. **93**, 5533 (1990).
[27] L. B. Knight, Jr., W. C. Easley, W. Weltner, Jr., and M. Wilson, J. Chem. Phys. **54**, 322 (1971).
[28] IODINESPEC4, Toptica Photonics, Munich, Germany (www.toptica.com).
[29] A. L. Schawlow, Rev. Mod. Phys. **54**, 697 (1982).
[30] G. Herzberg, *Molecular Spectra and Molecular Structure* (Van Nostrand Reinhold Company, New York, 1950).
[31] J. M. Brown and A. Carrington, *Rotational Spectroscopy of Diatomic Molecules* (Cambridge University Press, Cambridge, England, 2003).
[32] K. P. Huber and G. Herzberg, *Molecular Spectra and Molecular Structure: IV Constant of Diatomic Molecules* (Van Nostrand Reinhold Company, New York, 1979).
[33] W. Weltner, Jr., *Magnetic Atoms and Molecules* (Dover, New York, 1983).
[34] A. R. Edmonds, *Angular Momentum in Quantum Mechanics* (Princeton University Press, Princeton, NJ, 1960).